Momentum Distribution of ^{15}B Fragments from the Breakup of ^{17}B

T. Suzuki,[1] Y. Ogawa,[2] M. Chiba,[3,4] M. Fukuda,[2] N. Iwasa,[3] T. Izumikawa,[5] R. Kanungo,[4] Y. Kawamura,[1] A. Ozawa,[4] T. Suda,[4] I. Tanihata,[4] S. Watanabe,[1] T. Yamaguchi,[4] and Y. Yamaguchi[1,4]

[1]*Department of Physics, Niigata University, Niigata 950-2181, Japan*
[2]*Department of Physics, Osaka University, Osaka 560-0043, Japan*
[3]*Department of Physics, Tohoku University, Miyagi 980-8678, Japan*
[4]*The Institute for Physical and Chemical Research (RIKEN), Wako, Saitama 351-0198, Japan*
[5]*Radio-Isotope Center, Niigata University, Niigata 951-8518, Japan*

(Received 25 December 2001; published 13 June 2002)

The two-neutron removal cross section (σ_{-2n}) and the longitudinal momentum distribution of ^{15}B fragments from the breakup of ^{17}B on ^{9}Be were measured at 70A MeV. The distribution in the projectile rest frame is characterized by a FWHM of 80 $\pm$ 10 MeV/c for ^{15}B. The σ_{-2n} is found to be 0.22 $\pm$ 0.05 b. A Glauber–type analysis of the data provides clear evidence of a two-neutron halo structure in ^{17}B.

DOI: 10.1103/PhysRevLett.89.012501 PACS numbers: 21.10.Gv, 25.60.Gc, 27.20.+n

It is well-known that some nuclei far from stability develop a structure with a dilute matter distribution that extends very far beyond the core of the nucleus. Such structures are well described by a core, resembling a normal nucleus, surrounded by an extended valence nucleon or nucleons, and are referred to as nuclear halos [1]. In general terms, the halo may be regarded as a threshold phenomenon. A very loosely bound valence nucleon or nucleons held in short-range potential wells can tunnel into the surrounding space with significant probability to be present at distances much larger than the nuclear radius. The development of the halo is governed by the separation energy of the valence nucleon(s) and the reduced mass of the system [2] as well as the centrifugal barrier [3].

Halo nuclei are characterized by weak binding of the last bound nucleon (or nucleons), large reaction cross sections, large rms matter radii, and narrow momentum distributions following fragmentation and concentration of the dipole breakup strengths at low continuum energies. These features are most clearly seen for the last two neutrons in ^{6}He, and ^{11}Li and for the last neutron in ^{11}Be, and ^{19}C. The neutron-rich nuclei ^{14}Be and ^{17}B have been considered to be "candidate" halo systems since the observation of their large matter radii [4]. ^{17}B has bulk properties similar to those of ^{14}Be. The matter radius [5] and the two-neutron separation energy (S_{2n}) [6] are reported to be 3.10 $\pm$ 0.15 fm, 1.34 $\pm$ 0.11 MeV for ^{14}Be, and 2.99 $\pm$ 0.09 fm, 1.39 $\pm$ 0.14 MeV for ^{17}B. The radii of ^{14}Be and ^{17}B are much larger than those of ^{12}Be (2.59 $\pm$ 0.06 fm [4]) and ^{15}B (2.59 $\pm$ 0.03 fm [7]).

Both the angular distribution of neutrons [8] and the longitudinal momentum distribution [9] of ^{12}Be produced by the breakup of ^{14}Be exhibit narrow widths suggestive of a halo structure in ^{14}Be. Recently, an experiment for ^{14}Be was performed by Labiche *et al.* [10]. The two-neutron removal cross section (σ_{-2n}), neutron angular distributions and invariant mass spectra characteristic of a halo structure were observed, thus establishing a halo structure in ^{14}Be. However, little is known about ^{17}B beyond its matter radius, and therefore it is important to measure the longitudinal momentum ($p_{\parallel}$) distribution for ^{15}B fragments from the breakup of ^{17}B [11], in order to obtain more detailed structure information. In this Letter we report on new results obtained from measurements at the Riken Projectile Fragment Separator (RIPS) [12], of the $p_{\parallel}$ distribution and σ_{-2n} of ^{17}B after breakup on a Be target at 70A MeV incident energy.

The ^{17}B beam ($\sim$30 pps) was delivered from the RIPS, as follows. A 110A MeV ^{22}Ne primary beam was used to bombard a Be (920 mg/cm^2) production target. The emittance for the secondary beam was restricted to be $\pm$20 mrad in both the horizontal and vertical directions by a set of collimators, which was placed 40 cm downstream from the production target so as not to affect the final momentum acceptance for ^{15}B. A thick, wedge-shaped Al degrader (average thickness of 1638 mg/cm^2 and average slope of 8.67 mrad) was placed at the first focal plane (F1) of the RIPS. The momentum spread in a beam of $\pm$0.25%, determined by the slit at F1, was measured by the time-of-flight (TOF) between plastic scintillators (0.5 mm thick) located at F1 and at the achromatic focus (F2). The distance between these foci was 10.8 m. Particles were identified by the $B\rho$-TOF-ΔE technique. The energy loss was measured in a Si detector (350 μm thick) at F2 as well as in the scintillators. Additionally, the TOF with the rf signal from the accelerator was used. The impurity in the ^{17}B beam was reduced to less than one part in 10^5 in the off-line analysis. The mean energy of the beam was 70A MeV at the midpoint of the secondary reaction target (Be; 277 mg/cm^2 $\times$ 30$_{mm}\phi$) placed at F2. The beam position at the reaction target was restricted by a collimator ($\pm$10 mm) located 10 cm upstream from the reaction target, and was measured by a parallel-plate avalanche counter (PPAC).

The charged fragments from the breakup were transported to the final focus (F3) through triplet Q magnets, of which the characteristics are summarized in Table 4 of Ref. [12], located 1.5 m downstream from the reaction

target with an opening size of 17.2 cm ϕ. Particles were tracked by PPACs and identified using a large-area Si-NaI telescope (three layers of Si 5×5 cm$^2 \times 500$ μm, and NaI $3'' \phi \times 6$ cm). The velocity of a fragment was determined by the TOF between F2 and F3 with a path length of 6.0 m. A TOF calibration was performed for section F1-F2 using primary beams with energies of 110A, 84.6A, and 59.8A MeV and for section F2-F3 by changing the magnetic field of the second dipole magnet by $\pm 2.5\%$ so as to obtain a different velocity (β) for ^{17}B, since the magnetic rigidity is proportional to the velocity for a particle with a given mass-to-charge ratio. The total momentum resolution of the system was 33 MeV/c (0.6%) in FWHM or 14 MeV/c in σ (Fig. 1a).

This resolution is sufficient to accurately measure $p_{\|}$ distribution widths as narrow as that observed for ^{11}Li ($\sim$44 MeV/c [13]). Furthermore, the large transmission of section F2-F3 provides for minimal distortion of the measured distribution. The transmission for ^{15}B was calculated using the simulation code MOCADI [14], assuming a three-dimensional Lorentzian line shape with $\Gamma \sim 80 \pm 10$ MeV/c that is close to the observed line shape, and was found to be 80($\mp$5)%. Most of the loss was due to the angular spread at the target. The acceptance due to the finite sizes of the detectors at F3 was found to be 82(5)%. This was estimated using MOCADI with and without a gate on the positions at F3, where the gate was the same as that used in the off-line analysis. Note that the transmission does not depend on the momentum of ^{15}B within a range of $\pm \Delta p/p \sim 2\%$, which is larger than the measurement range of $\pm 1.7\%$.

The energy response of the telescope was calibrated under the magnet setting for $A/Z = 3$ particles. Data were also acquired without the Be breakup target by reducing the beam energy by an amount corresponding to the energy loss in the target. The empty-target data were used to subtract events arising from reactions in the telescope. Figure 1b shows the energy spectrum in the NaI detector from ^{9}Be + ^{17}B reactions with and without the breakup target. One can clearly see the peak of ^{15}B, which we attribute to the dissociation of ^{17}B. The TOF, which gives the total momentum (p), and is very close to $p_{\|}$ within the resolution, was converted to $p_{\|}$ in the projectile rest frame for both target-in and empty-target runs, after selecting the ^{15}B in the NaI energy spectrum, as indicated by the arrow in Fig. 1b. The signal-to-noise ratio in the ^{15}B gate was 1.3. The peak position in the $p_{\|}$ spectrum for the target-in run was shifted relative to that for the empty-target run by +70 MeV/c, which is known to be due to the momentum transfer to the target [15].

The background-subtracted $p_{\|}$ spectrum is shown in Fig. 2a. The experimental data points [$N(p_{\mathrm{i}})$] in the figure were normalized to the measured σ_{-2n} value, described below, so as to be $\sum N(p_{\mathrm{i}}) \Delta p_{\|} = \sigma_{-2n}$. The error bars do not include the uncertainty (22%) in the measured σ_{-2n} value. The deduced $p_{\|}$ distribution was fitted with a Lorentzian, $[\Gamma/2]^2/(p^2 + [\Gamma/2]^2)$, with width $\Gamma = 86 \pm$

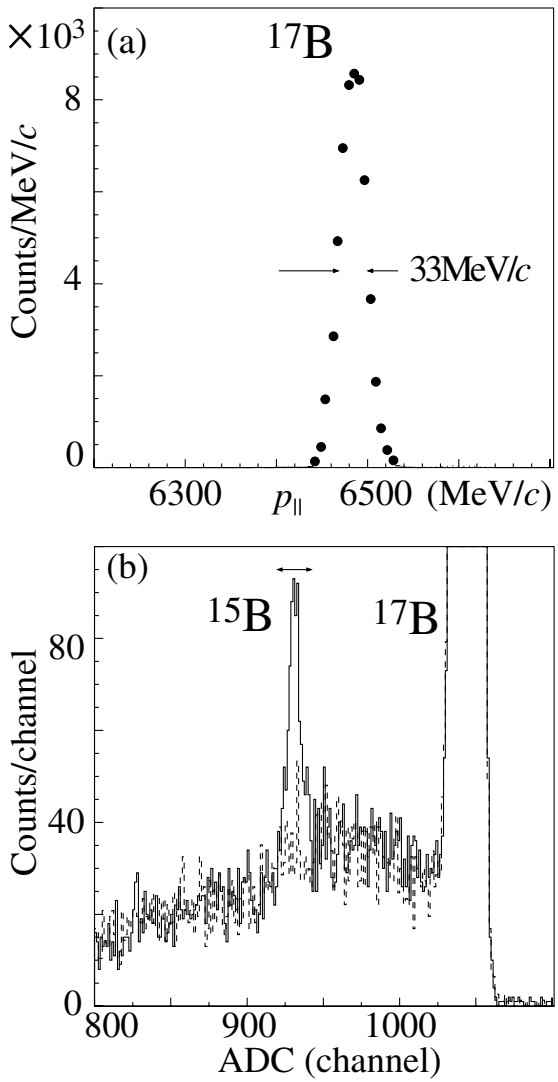

FIG. 1. (a) Momentum spectrum for ^{17}B + Be $\rightarrow$ ^{17}B from TOF. The momentum resolution of the system (33 MeV/c FWHM) was determined from the width of the ^{17}B peak. (b) Number of events in the NaI detector, obtained via a charge-sensitive ADC corrected using TOF, for ^{17}B reacting in a Be target. The solid line is the total spectrum, where the peak from the transmitted ^{17}B is off scale; the dashed line is for the empty-target run. The produced ^{15}B is clearly seen above the background due to reactions in the NaI detector. The arrow indicates the gate for ^{15}B.

10 MeV/c, as indicated by the dashed curve in Fig. 2a. By unfolding the system resolution of $\sigma = 14$ MeV/c, the width was found to be 80 ± 10 MeV/c. The width is as narrow as that observed in ^{14}Be $\rightarrow$ ^{12}Be fragmentation [9] (88 ± 5 MeV/c). In simple terms the narrow width corresponds, via the uncertainty principle, to an extended spatial distribution for the valence neutrons of ^{17}B. The width of the distribution is discussed below.

The σ_{-2n} was deduced while taking into account the transmission of ^{15}B for section F2-F3 and the detector acceptance at F3, as mentioned previously. It should be noted here that the calculated F2-F3 transmission for ^{17}B, including the acceptance under the magnet setting for ^{15}B, was

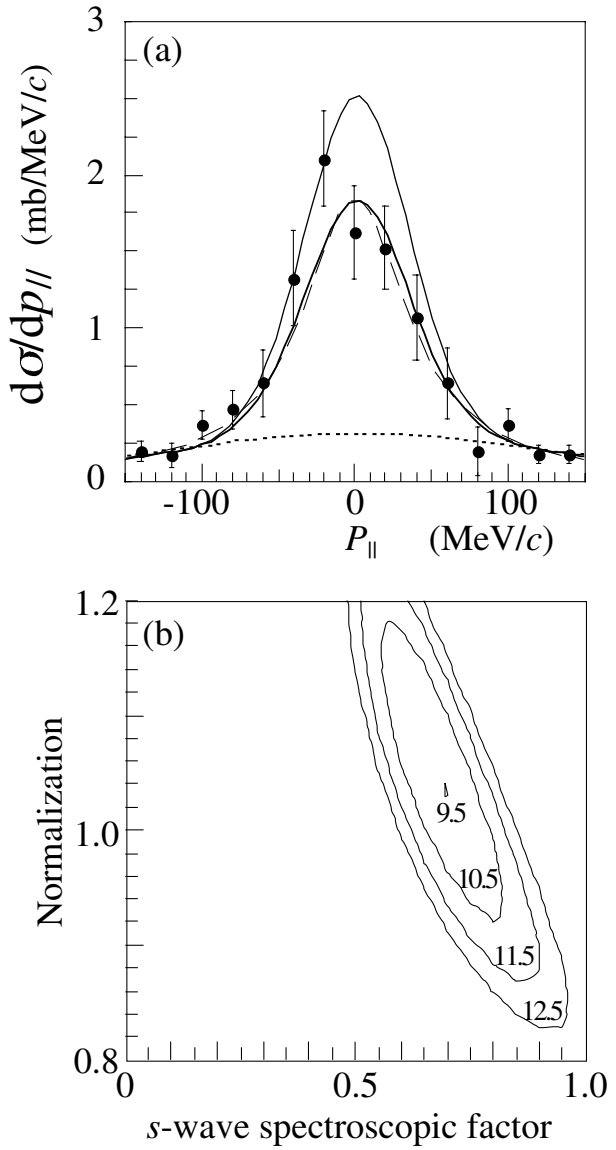

FIG. 2. (a) ^{15}B longitudinal momentum distribution from ^{17}B fragmentation on ^{9}Be in the projectile rest frame at 70A MeV. The experimental data points $N(p_i)$ are normalized to the measured σ_{-2n} value so that $\sum N(p_i)\Delta p_{\parallel} = \sigma_{-2n}$. The error bars do not include the uncertainty in the normalization. The theoretical curves were folded with a Gaussian resolution function having $\sigma \sim 14$ MeV/c. The solid and dotted curves represent the results for pure $2s_{1/2}$ and $1d_{5/2}$ waves, respectively. The thick-solid curve indicates the result with a s-wave spectroscopic factor of 0.69. The dashed curve shows a Lorentzian with $\Gamma = 86.3$ MeV/c (see text for details). (b) The contour plot of χ^2 values as a function of the s-wave spectroscopic factor and the normalization. The corresponding χ^2 value is indicated at each contour line.

45%, consistent with the experimental data, i.e., the ratio of the number of ^{17}B at F3 (tracking efficiency corrected) divided by that at F2 within an accuracy of 5%. Thus, we estimated the systematic error resulting from the F2-F3 transmission to be about 5%. The σ_{-2n} was also measured by putting the breakup target just in front of the Si-NaI telescope to avoid any uncertainty in the transmission and the acceptance. The two methods give consistent values, 0.23 ± 0.04 b for target at F2 and 0.19 ± 0.08 b for target at F3, resulting in $\sigma_{-2n} = 0.22 \pm 0.05$ b at 70A MeV, where the experimental uncertainty includes both statistical and systematic errors.

The σ_{-2n} value is comparable with the result of few-body Glauber-type calculations [16,17]. A single neutron wave function [$\psi_j(\mathbf{r})$] was constructed with a Woods-Saxon potential, whose depth was chosen so as to reproduce $S_{2n}/2$ MeV, with the diffuseness parameter (α_0) of the binding potential chosen to be 0.7 fm and a radius parameter of $1.2A^{1/3}$ fm. We chose the total nucleon-nucleon cross section to be 70.6 mb, the zero-range limit, and $\alpha_{NN} = 1.02$ as the parametrized form for the profile function [18], which represents the absorption strength. We assumed the wave function of the two valence neutrons to be identical without any correlation between them in spite of the fact that ^{17}B is bound only due to nn pairing. As discussed later, we have introduced mixed $2s_{1/2}$ and $1d_{5/2}$ configurations. The present model reproduces the interaction cross section (σ_I) of ^{15,17}B on C at about 800A MeV (1000 $\pm$ 20 mb and 1118 $\pm$ 22 mb) [5,7] within an accuracy of a few percent. The reaction cross section (σ_R) of ^{15,17}B on ^{9}Be at 70A MeV was calculated to be 1079 and 1307 mb. Assuming the same magnitude of the inelastic cross section ($\sigma_{\rm inel}$) for both ^{15}B and ^{17}B, $\sigma_I(^{17}\mathrm{B}) - \sigma_I(^{15}\mathrm{B}) = \sigma_R(^{17}\mathrm{B}) - \sigma_R(^{15}\mathrm{B}) + \Delta\sigma_{\rm inel} = 0.23 \pm 0.03$ b, the difference satisfies the following relation [16]: $\sigma_I(^{17}\mathrm{B}) - \sigma_I(^{15}\mathrm{B}) = \sigma_{-2n}$, within the experimental uncertainty. This fact supports "a core plus two-neutron" structure in ^{17}B.

We also compared the observed $p_{\parallel}$ distribution with Glauber-type calculations [19–21]. The $p_{\parallel}$ distribution was calculated by using Eqs. (3.5)–(3.18) in Ref. [21]. We described the two-neutron removal reaction by two processes, depending on the final state of the target nucleus, the excited states or its ground state.

In the former process (often referred to as absorption), only one neutron collides with the target nucleus while the other neutron is removed by a free decay without forming a "^{15}B + n" resonance or stable ^{16}B excited states, and the core nucleus survives. In this process the momentum transfer received by the first neutron is significantly large. As for the second neutron separation, if the ^{16}B nucleus has a sharp resonance peak, the final-state interaction between the neutron and core nucleus would be important. A recent experiment [22], however, indicates that both the ground and first excited states of the ^{16}B nucleus have a width of the order of 100 keV, which is comparable with that of ^{10}Li [23], and does not show narrow resonance behavior. The ground state of ^{16}B is unbound by 40 ± 60 keV [22], of which the situation is also similar to that of ^{10}Li (unbound by less than 100 keV) [24]. Based on these facts, we assumed that the separation of the second neutron proceeds as a free decay. We therefore approximated the scattering wave of two neutrons with the plane wave.

In the latter process, where the target nucleus remains in its ground state, the two-neutron ground state (often

referred to as diffraction or elastic breakup) wave function is distorted by the phase-shift functions. The halo neutrons then decay into the continuum, which is determined by the $^{15}B + n + n$ three-body Hamiltonian, in principle. In this case the momentum transfer is small, and the final-state interaction would be important. The plane wave was modified so as to be orthogonal to the ground state in order to fulfill the minimum requirement of the outgoing wave of this elastic breakup process, and was used as the scattering wave to include this significant point.

While we modeled the breakup reaction as mentioned above, the wave function for the two valence neutrons was calculated assuming a "core plus $2n$" as the structure of ^{17}B. It is the same as that used in the calculation of σ_{-2n}. We considered the $(2s_{1/2})^2_{J=0}$ or $(1d_{5/2})^2_{J=0}$ configurations for the two valence neutrons, i.e., $\Phi(\mathbf{r}_1, \mathbf{r}_2) = [\psi_j(\mathbf{r}_1)\psi_j(\mathbf{r}_2)]_{J=0}$, where $j = 1d_{5/2}$ or $2s_{1/2}$. For simplicity we considered only the $J = 0$ configuration, in order to see whether the ^{17}B nucleus has a halo structure.

The results for pure $2s_{1/2}$ and for $1d_{5/2}$ are shown in Fig. 2a as the solid and dotted curves, respectively. A Gaussian resolution function having $\sigma \sim 14$ MeV/c is convoluted with the theoretical curves. It is clear that neither distribution for a pure configuration reproduces the experimental distribution. We next considered configuration mixing, i.e., taking

$$\Phi(\mathbf{r}_1, \mathbf{r}_2) = \sqrt{N}\{\sqrt{\lambda}[\psi_{2s_{1/2}}(\mathbf{r}_1)\psi_{2s_{1/2}}(\mathbf{r}_2)]_{J=0} + \sqrt{(1-\lambda)}[\psi_{1d_{5/2}}(\mathbf{r}_1)\psi_{1d_{5/2}}(\mathbf{r}_2)]_{J=0}\}$$

as the valence two-neutron wave function. We fit the data so as to minimize the χ^2 value, while taking both N and λ to be free parameters. The minimum χ^2 is at $N = 1.04 \pm 0.14$ and $\lambda = 0.69 \pm 0.14$, as can be seen in Fig. 2b. The thick-solid curve in Fig. 2a shows the result of the best fit. The FWHM of this distribution is 91 ± 10 MeV/c, including the system resolution and 80 ± 10 MeV/c without the system resolution.

The uncertainty of $\pm 22\%$ in the normalization of each experimental data point $N(p_i)$ changes the mixing ratio by $\pm 20\%$, as can be seen in Fig. 2b, which is larger than the error from the fitting of $\pm 14\%$. Thus, the s-wave spectroscopic factor (λ) is 0.69 ± 0.20. This value suggests a dominant s-wave contribution, and is larger than 0.36 ± 0.19 [5], which is reported to reproduce the observed σ_I of ^{17}B on C at 800A MeV, but is consistent with it, within the experimental uncertainties. We consider configuration mixing in the sd shell to be essential to explain the observed $p_{\|}$ distribution, together with σ_I or σ_R.

The rms radius of the Woods-Saxon wave function, which represents the rms distance between the relative motion of the core and the c.m. of two neutrons ($r_{c(nn)}$), is 4.66, 2.93, and 4.20 fm for the pure $2s_{1/2}$, $1d_{5/2}$, and the mixed case with $\lambda = 0.69$, respectively. The value of 4.20 fm together with the rms radius of ^{15}B gives the rms radius of ^{17}B to be 3.13(3) fm, which is slightly (4.7%) larger than the reported value of 2.99(9) fm [5]. Taking into account the experimental uncertainty in the s-wave spectroscopic factor, it ranges from 3.04(3) fm to 3.23(3) fm and is consistent with the reported value within the experimental uncertainties. The $r_{c(nn)}$ value is much larger than the size of ^{15}B, and thus suggests a structure for ^{17}B of a two-neutron halo surrounding a ^{15}B nucleus.

In summary, this Letter reports the first measurement of the ^{15}B longitudinal momentum distribution and two-neutron removal cross section for ^{17}B breakup. The two-neutron removal cross section of 0.22 ± 0.05 b is consistent with a "core plus two-neutron" picture in ^{17}B. The width of the $^{17}B \rightarrow {}^{15}B$ momentum distribution was found to be 80 ± 10 MeV/c, FWHM. A Glauber-type calculation with an adiabatic treatment of the two valence neutrons provides clear evidence of a two-neutron halo structure in ^{17}B.

The authors are indebted to the members of the Riken Accelerator staff for stable operation of the accelerator. We thank Dr. J. Miller at LBNL for his careful reading of the manuscript. This work was supported in part by the Japanese Ministry of Education, Science, Sports and Culture by Grant-In-Aid for Scientific Research under Program No. B(2) 13440075.

[1] P. G. Hansen *et al.,* Annu. Rev. Nucl. Part. Sci. **45**, 591 (1995).
[2] P. G. Hansen and B. Jonson, Europhys. Lett. **4**, 409 (1987).
[3] K. Riisager *et al.,* Nucl. Phys. **A548**, 393 (1993).
[4] I. Tanihata *et al.,* Phys. Lett. B **206**, 592 (1988); A. Ozawa *et al.,* Phys. Lett. B **334**, 18 (1994).
[5] T. Suzuki *et al.,* Nucl. Phys. **A658**, 313 (1999).
[6] G. Audi, O. Bersillon, J. Blachot, and A. H. Wapstra, Nucl. Phys. **A624**, 1 (1997).
[7] A. Ozawa *et al.,* Nucl. Phys. **A608**, 63 (1996).
[8] K. Riisager *et al.,* Nucl. Phys. **A540**, 365 (1992).
[9] M. Zahar *et al.,* Phys. Rev. C **48**, R1484 (1993).
[10] M. Labiche *et al.,* Phys. Rev. Lett. **86**, 600 (2001).
[11] I. Tanihata, J. Phys. G. **22**, 157 (1996).
[12] T. Kubo *et al.,* Nucl. Instrum. Methods Phys. Res., Sect. B **70**, 309 (1992).
[13] N. Orr *et al.,* Phys. Rev. Lett. **69**, 2050 (1992).
[14] N. Iwasa *et al.,* Nucl. Instrum. Methods Phys. Res., Sect. B **126**, 284 (1997).
[15] S. B. Kaufman *et al.,* Phys. Rev. C **26**, R2694 (1982).
[16] Y. Ogawa, K. Yabana, and Y. Suzuki, Nucl. Phys. **A543**, 722 (1992).
[17] J. S. Al-Khalili, J. A. Tostevin, and I. J. Thompson, Phys. Rev. C **54**, 1843 (1996).
[18] S. M. Lenzi, A. Vitturi, and F. Zardi, Phys. Rev. C **40**, 2114 (1989).
[19] J. Hüfner and M. C. Nemes, Phys. Rev. C **23**, 2538 (1981).
[20] Y. Ogawa, Y. Suzuki, and K. Yabana, Nucl. Phys. **A571**, 784 (1994).
[21] Y. Ogawa, T. Kido, K. Yabana, and Y. Suzuki, Prog. Theor. Phys. Suppl. **142**, 157 (2001).
[22] R. Kalpakchieva *et al.,* Eur. Phys. J. A **7**, 451 (2000).
[23] W. Benenson, Nucl. Phys. **A588**, 11 (1995).
[24] B. M. Young *et al.,* Phys. Rev. C **49**, 279 (1994).